2024 IEEE 35th International Symposium on Personal, Indoor and Mobile Radio Communications (PIMRC) | 979-8-3503-6224-4/24/$31.00 ©2024 IEEE | DOI: 10.1109/PIMRC59610.2024.10817190

Simultaneous Interference Graph Estimation and Resource Allocation in Multi-Cell Multi-Numerology Networks

Daqian Ding[1], Wei Lou[2], Hong Hu[2], Haorui Li[1], and Yibo Pi[1]

[1]Shanghai Jiao Tong University, Shanghai, China
[2]East China Branch of State Grid Corporation of China, Shanghai, China
Email: yibo.pi@sjtu.edu.cn

***Abstract*—Resource allocation in multi-cell networks typically requires knowing the inter-cell interference channel gains. When multiple numerologies are employed, resource allocation further needs to estimate the inter-numerology interference within each cell. However, there lacks viable methods of interference graph estimation (IGE), depicting the intra- and inter-cell interference channel gains, for multi-cell multi-numerology networks. To fill this gap, we propose an efficient power-domain approach to IGE for the resource allocation in multi-cell multi-numerology networks. Unlike traditional reference signal-based approaches that consume frequency-time resources, our approach uses power as a new dimension for the estimation of channel gains. By carefully controlling the transmit powers of base stations, our approach is capable of estimating both the intra- and inter-cell interference channel gains, useful to resource allocation. Further, as a power-domain approach, it can be seamlessly integrated with the resource allocation in multi-numerology networks, such that IGE and resource allocation can be conducted simultaneously. We derive the necessary conditions for power-domain IGE and formulate the joint optimization problem of IGE and resource allocation. Our simulation results show that power-domain IGE can accurately estimate the interference channel gains and incurs low power overhead.**

I. Introduction

With the goal of supporting diverse services, the 5G new radio (NR) systems introduce multi-numerology (MN) that allows flexible selection of frame structure based on service requirements. Frames with large subcarrier spacing (SCS) may be employed for users with strict latency requirements and frames with small SCS are preferable for users with highly frequency-selective channels. The flexibility of multi-numerology enables 5G to simultaneously support services of different requirements. However, the use of multiple numerologies also incurs the inter-numerology interference (INI) between different numerologies. In contrast to single-numerology networks, the presence of INI greatly complicates the interference management in MN networks. Each user equipment (UE) may experience not only interference from neighboring cells on its assigned frequency band but also INI from other frequency bands in both the serving and neighboring cells. It is thus critical to manage INI for the performance of MN networks.

Effective INI management can be achieved by optimizing the MN system from different angles. From the perspective of system design, many design parameters, e.g., waveform, guard band, and cyclic prefix (CP), can be considered. New waveforms have been proposed for several typical subband filtered multi-carrier (SFMC) based systems to reduce the out-of-band emission level, including filter-band multi-carrier [1], [2], universal filtered multi-carrier [3], generalized frequency division multiplexing [4], and filtered OFDM [5]. Large guard bands and long CPs are shown to effectively mitigate INI at the cost of spectral efficiency [6], [7]. When the system design is fixed, we can further mitigate INI with resource allocation [8]–[10], which emphasizes the proper allocation of power and frequency-time resources to guarantee certain service requirements. In multi-cell MN networks, both the INI within the cell (intra-cell INI) and the INI between neighboring cells (inter-cell INI) need to be considered.

The interference graph, depicting the intra- and inter-cell interference channel gains, is a powerful tool to guide resource allocation for interference management. Existing works on resource allocation in multi-cell MN networks typically assume knowing the interference graph and focus on developing resource allocation algorithms. However, interference graph estimation (IGE) is a challenging and heavy measurement task, because it requires estimating the channel gains between each pair of UE and interferer. In a network of N cells, each UE needs to consider $O(N)$ inter-cell interference links in single-numerology networks. In MN networks, if each cell uses M numerologies and that both intra- and inter-cell INIs exist, each UE may experience INI from $O(MN)$ sources of interference. It is therefore of paramount importance to efficiently estimate the interference graph.

INI models have been derived and used to estimate the interference in various MN systems. In [11]–[13], the closed-form expressions for intra-cell INI have been derived in the windowed OFDM, SFMC, and massive MIMO-OFDM systems for interference cancellation at the receiver, respectively. In [14], the expression for INI has been used to suppress intra-cell INI with precoding at the transmitter in the downlink of massive MIMO-OFDM systems. These theoretical expressions

979-8-3503-6224-4/24/$31.00 ©2024 IEEE

for INI assume the absence of system imperfections, e.g., time synchronization error and phase noise, and may not be applicable when practical issues are considered [12], [15]. In resource allocation problems, the power of interference channels needs to be modelled and used to calculate the signal-to-interference-plus-noise ratio (SINR). The intra-cell INI is simply modelled without involving the channel responses in [10] and the inter-cell INI is simply modelled as the product of the intra-cell INI and the inter-cell channel responses in [16]. These simplified models cannot reflect the INI in real systems and may significantly affect the performance of resource allocation when used in practice.

Compared to the model-based approaches above, reference signal (RS)-based approaches can accurately measure interference channel gains. In single-numerology systems, the most practical approach to measuring inter-cell interference is introduced in 4G LTE-A using the CSI-IM reference signal [17]. Specifically, in order to measure the inter-cell interference from a BS to a UE on a specific resource element (RE), other BSs should send no signal on that RE. The signal UE receives on the RE will then be the interference from the BS. This process is repeated for each BS to construct the interference graph from BSs to UEs. However, this approach requires symbol-level synchronization between BSs for accurate estimation of the interference channels. With the increasing subcarrier spacing in 5G NR, the CP duration decreases to the millisecond level, making this approach susceptible to synchronization error [18]. Furthermore, this approach consumes frequency-time resources solely for measurement purposes, and frequent measurements may incur non-negligible overhead. Using reference signals for IGE in MN networks faces the same issues above. Moreover, it is unclear how to use reference signals to measure inter-cell interference in MN networks.

Considering the heavy measurement overhead of IGE, machine learning approaches have been proposed to build a direct mapping from network attributes to resource allocation decisions, without explicitly measuring interference. Geographic information of nodes have been used as input to learn the link scheduling decisions from a large scale of layouts in device-to-device networks [19]. With graph embedding, the same task for link scheduling can be achieved using hundreds of times fewer layouts for training [20]. These machine learning techniques do not need explicit interference measurement, but their dependence on static network attributes constrains their ability to adapt to rapidly changing network conditions.

Our focus in this paper is on the estimation of interference graph for resource allocation in the downlink of OFDMA-based multi-cell MN networks. Specifically, we want to 1) estimate the interference graph including both the intra- and inter-cell interference channels and 2) use the estimated interference graph to improve the energy efficiency of the system. We propose a power-domain approach to IGE that estimates the interference graph by manipulating the transmit power of BSs, such that the frequency-time resources can be simultaneously used for measurement and data transmission tasks. Our core insight is that the expected receive power of a UE at a time slot can be written as a linear combination of the transmit powers of BSs and the channel gains. By combining the receive powers of the UE at different time slots, a group of equations for the same set of channel gains can be obtained to derive a unique solution for IGE. With the estimated intra- and inter-cell channel gains, we can formulate a resource allocation problem aiming to maximize energy efficiency and estimate interference channel gains simultaneously.

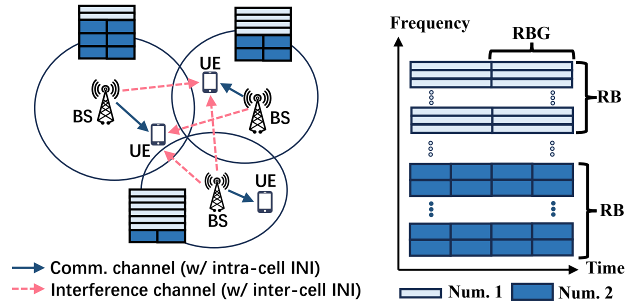

(a) Network architecture (b) Frame structure

Fig. 1. A multi-cell multi-numerology network

In summary, our contributions in this paper are as follows.

- We propose to estimate the interference graph in the power domain by manipulating the transmit powers of BSs, robust to timing offsets.
- We formulate the joint optimization problem of resource allocation and IGE for multi-cell multi-numerology systems, such that IGE and resource allocation can be done simultaneously using the same frequency-time resources.
- We demonstrate with simulations that our approach can accomplish resource allocation and IGE simultaneously with low overhead in power consumption.

II. System Model

A. Multi-Cell Multi-Numerology Networks

We consider the downlink of a multi-cell OFDMA network with K BSs, which are connected to the core network via either a fiber or wireless backhaul (Figure 1(a)). Each UE is associated with one BS, and BSs serve each of its associated UEs with one numerology and use multiple numerologies to provide diverse access services. For spectrum efficiency, each BS re-uses the same frequency-time resources and UEs receive the inter-cell interference from neighboring BSs. Each UE experiences multiple sources of interference: 1) intra-cell INI in the communication channel, due to the non-orthogonality between different numerologies used by the BS, 2) inter-cell co-channel interference from neighboring cells in the same frequency, and 3) inter-cell INI from neighboring cells in other frequency bands using different numerologies. To mitigate interference, BSs efficiently coordinate resource allocation such that the demands of UEs are satisfied. In this paper, we consider the timing offset (TO) and carrier frequency offset (CFO) of the received signal at the UEs. The CFO is caused by the oscillator mismatch in frequency and the TO is caused by the time synchronization errors between BSs as well as the differences in propagation delay from BSs to the UE.

Let $\mathcal{I} = \{0, \ldots, I\}$ be the total numerology set and $\mathcal{I}_k \subseteq \mathcal{I}$ be the numerology set used by BS k, where numerology 0 has the narrowest SCS. Let Δf^i be the SCS of numerology i, and N^i and N^i_{cp} be the lengths of the OFDM symbols and CPs corresponding to numerology i. Following the standard design in 5G NR [21], we relate the SCSs, the lengths of OFDM symbols and CPs between numerologies as

$$\frac{N^i}{N^0} = \frac{N^i_{cp}}{N^0_{cp}} = \frac{\Delta f^0}{\Delta f^i} = \frac{1}{2^i}. \tag{1}$$

Figure 1(b) shows the frame structure of the resource grid with two numerologies following the above relations. Each resource block (RB) consists of 12 subcarriers and lasts for one OFDM symbol time. Consecutive RBs are combined into RB groups (RBGs), which are the least common multiple of the symbol durations across all numerologies. Since the RBGs of different numerologies are aligned in time, we can flexibly schedule resources at the RBG level.

B. Channel Model

The n-th sample of the time-domain transmitted signal from BS k is denoted as $x_k[n]$, which is the combined signal of the numerologies in $\mathcal{I}_k$. We can express $x_k[n]$ as $x_k[n] = \sum_{i \in \mathcal{I}_k} x^i_k[n]$, where $x^i[n]$ is the signal of numerology i. Let $X^i_k[m]$ be the symbol transmitted over the m-th subcarrier using numerology i and $\mathcal{Z}^i_k$ be the set of RBs using numerology i, where these RBs are not necessarily contiguous. Setting $X^i_k[m]$ to zero for subcarriers not in the RBs in $\mathcal{Z}^i_k$, we can simply write $x^i_k[n]$ as

$$x^i_k[n] = \frac{1}{\sqrt{N^i}} \sum_{m=0}^{N^i-1} X^i_k[m] e^{j2\pi mn/N^i}.$$

We denote the CFO of BS k as ω_k, normalized to the subcarrier spacing, and the synchronization error as ζ_k. Suppose the channel from BS k to UEs is an independent L-tap multipath fading channel. The n-th sample in the time-domain received signal of UE z can be expressed as

$$y_z[n] = \sum_{k \in \mathcal{K}} e^{j2\pi n\omega_k/N^i_{k,z}} \sum_{l=0}^{L-1} h^{(l)}_{k,z} x_k[n - l - \zeta_k] + v[n], \tag{2}$$

where $N^i_{k,z}$ is the number of subcarriers of UE z in BS k using numerology i, $h^{(l)}_{k,z}$ is the l-th channel tap from BS k to node z, and $v[n]$ is the zero-mean additive Guassian noise with variance σ_v^2.

III. Interference Graph Estimation: A Power-Domain Approach

Let T_{LCM} be the symbol duration of the numerology with the narrowest SCS, i.e., the duration of RGBs, and T_i be the symbol duration of numerology i. Based on the numerology properties in Eq. (1), we then have $T_{LCM} = 2^i T_i$, where numerology 0 has the narrowest SCS.

Lemma 1. *For the downlink of the OFDMA-based multi-cell multi-numerology systems, if $\mathbb{E}[X^i_k[m]] = 0$ for all k's and i's, the expected receive power of UE z on the d-th subcarrier is a linear combination of the equivalent channel gains and the expected transmit powers of BSs on subcarriers, i.e.,*

$$2^i \hat{p}^i_{z,rx}[d] = \sum_{k \in \mathcal{K}} \sum_{j \in \mathcal{I}_k} \sum_{m=0}^{N^j-1} 2^j \hat{p}^j_{k,tx}[m] s^{j \to i}_{(k,m),(z,d)} + \hat{V}_z[d],$$

where $\hat{p}^i_{z,rx}[d] = \mathbb{E}[|Y^i_z[d]|^2]$ is the receive power of UE z on the d-th subcarrier using numerology i, $\hat{p}^i_{k,tx}[m] = \mathbb{E}[|X^j_k[m]|^2]$ is the transmit power of BS k on the m-th subcarrier using numerology j, $\hat{s}^{j \to i}_{(k,m),(z,d)}$ is the equivalent channel gain from the m-th subcarrier of BS k to the d-th subcarrier of UE z, and $\hat{V}_z[d]$ is the noise power on subcarrier d of UE z.

Proof: Please refer to Appendix A. ■

Lemma 1 indicates the relation between power and channel gains at the subcarrier level. Considering that OFDMA-based systems allocate resources at the resource block (RB) level, we want to aggregate subcarriers into RBs of B subcarriers. Let $\mathcal{RB}_k$ be the set of RBs used by BS k and μ_d be the numerology of RB d. By summing up the receive powers on subcarriers in a RB, we can have the following corollary.

Corollary 1. *The expected receive power of UE on the d-th RB is a linear combination of the equivalent channel gains and the expected transmit powers of BSs on RBs, i.e.,*

$$2^{\mu_d} p^{rx}_z[d] = \sum_{k \in \mathcal{K}} \sum_{j \in \mathcal{RB}_k} 2^{\mu_j} p^{tx}_k[j] s_{(k,j),(z,d)} + V_z[d],$$

where $p^{rx}_z[d] = \sum_{j=B(d-1)+1}^{Bd} \hat{p}^{\mu_j}_{z,rx}[j]$ is the receive power of UE z on the d-th RB, $p^{tx}_k[j] = B\hat{p}^{\mu_j}_{k,tx}[j]$ is the transmit power of BS k on the j-th RB, $s_{(k,j),(z,d)} = \frac{1}{B} \sum_{j=B(d-1)+1}^{Bd} \hat{s}^{\mu_j \to \mu_d}_{(k,j),(z,d)}$, and $V_z[d] = \sum_{j=B(d-1)+1}^{Bd} \hat{V}_z[j]$.

Based on Corollary 1, we can derive the necessary conditions for achieving IGE with power control. We assume that the total number of RBs involved in the multi-cell MN networks is N_{RB} with indices from 1 to N_{RB}.

Theorem 1. *The equivalent channel gains on different RBs from BSs to UEs can be uniquely determined by controlling the transmit powers of BSs on RBs over time such that*

$$rank(\mathbf{P}) = N_{RB}, \tag{3}$$

where $\mathbf{P} = \left[\mathbf{p}^{tx}_1, \ldots, \mathbf{p}^{tx}_{N_{RB}}\right]$ is the transmit power matrix of BSs, $\mathbf{p}^{tx}_i = [2^{\mu_i} p^{tx}_i[j], \ldots, 2^{\mu_i} p^{tx}_i[j+n-1]]^T$ includes the transmit powers on the i-th RB from time j to $j+n-1$, and μ_i is the numerology of RB i.

Proof: Let $s_{d,i}$ be the equivalent channel gain from RB d of the BS to RB i of the UE. Suppose that a UE receives on RB i with the receive power vector, denoted as $\mathbf{p}^{rx}_i = [2^{\mu_i} p^{rx}_i[j], \ldots, 2^{\mu_i} p^{rx}_i[j+n-1]]^T$. We can have that

$$\mathbf{p}^{rx}_i = \mathbf{P}\mathbf{s}_i + \mathbf{v},$$

where $\mathbf{s}_i = [s_{1,i}, \ldots, s_{N_{RB},i}]^T$ and $\mathbf{v} = [V[j], \ldots, V[j+n-1]]^T$ is the vector of noise power. If the transmit power matrix $\mathbf{P}$ is full-rank, we can then have a unique solution for $\mathbf{s}_i$. ■

IV. Joint Optimization for Interference Graph Estimation and Resource Allocation

A. Problem Formulation

Our goal is to 1) maximize the energy efficiency of the multi-cell MN system under the constraint that user traffic demand is satisfied and 2) estimate the interference graph with power control simultaneously. Let $\mathcal{U}_k$ be the set of UEs served by BS k, and $\mathcal{T}$ be the set of time blocks. We define network energy efficiency following the definition in [22] as

$$E(\mathbf{P}) = \frac{f(\mathbf{P})}{g(\mathbf{P})} = \frac{\sum\limits_{k\in\mathcal{K}}\sum\limits_{z\in\mathcal{U}_k}\sum\limits_{d\in\mathcal{RB}_k}\sum\limits_{l\in\mathcal{T}} log(1+\text{SINR}_{k,z}[d][l])}{\sum\limits_{k\in\mathcal{K}}\sum\limits_{z\in\mathcal{U}_k}\sum\limits_{d\in\mathcal{RB}_k}\sum\limits_{l\in\mathcal{T}} p_k^{tx}[d][l]},$$

where $p_k^{tx}[d][l]$ is the transmit power of BS k on RB d at the l-th time block and $\text{SINR}_{k,z}[d][l]$ denotes the signal-to-interference-plus-noise ratio of UE z served by BS k on RB d at time block l. Let $\delta_{k,z}[d][l]$ indicate if BS k is sending to UE z on RB d at the l-th time block and $p_{k,z}^{tx}[d][l]$ be the transmit power of BS k to UE z on RB d at time block l, where $p_{k,z}^{tx}[d][l] = 0$ if $\delta_{k,z}[d][l] = 0$. We have $p_k^{tx}[d][l] = \sum_{z\in\mathcal{U}_k} p_{k,z}^{tx}[d][l]$ and express the SINR as

$$\text{SINR}_{k,z}[d][l] = \frac{p_{k,z}^{tx}[d][l]s_{(k,d),(z,d)}}{\sum\limits_{\substack{k'\in\mathcal{K},\\ d'\in\mathcal{RB}_{k'}}} p_{k'}^{tx}[d'][l]s_{(k',d'),(z,d)} - p_{k,z}^{tx}[d][l]s_{(k,d),(z,d)} + V_{k,z}[d]},$$

where $V_{k,z}[d]$ is the noise power on RB d of UE z under BS k. The joint optimization problem can be formulated as

$$\begin{aligned}
(\mathcal{P}1)\ \max_{\mathbf{P},\boldsymbol{\delta}}\ & E(\mathbf{P}) \\
\text{s.t. }& (C_1)\ \sum_{z\in\mathcal{U}_k}\delta_{k,z}[d][l] \le 1, \forall k,d,l, \\
& (C_2)\ \sum_{d\in\mathcal{RB}_k}\delta_{k,z}[d][l] \ge 1, \forall k,z,l, \\
& (C_3)\ \delta_{k,z}[d][l] \in \{0,1\}, \forall k,z, \\
& (C_4)\ \text{SINR}_{k,z}[d][l] \ge \gamma_{k,z}\delta_{k,z}[d][l], \forall k,z, \\
& (C_5)\ 0 \le p_{k,z}^{tx}[d][l] \le \delta_{k,z}[d][l]P_{k,z}^{max}, \forall k,z, \\
& (C_6)\ 0 \le \sum_{z\in\mathcal{U}_k}\sum_{d\in\mathcal{RB}_k} p_{k,z}^{tx}[d][l] \le P_k^{max}, \forall k,l, \\
& (C_7)\ rank(\mathbf{P}) = N_{RB},
\end{aligned}$$

where $\gamma_{k,z}$ is the required SINR for UE z under BS k, $P_{k,z}^{max}$ is the maximum transmit power for UE z under BS k, and P_k^{max} is the maximum total transmit power of BS k.

B. Proposed Solution

$\mathcal{P}1$ is a rank-constrained mixed-integer nonlinear programming (MINLP) problem. We solve $\mathcal{P}1$ by dividing it into two sub-problems: an MINLP problem without the rank constraint,

$$\begin{aligned}
(\mathcal{P}2)\ \max_{\boldsymbol{P},\boldsymbol{\delta}}\ & E(\mathbf{P}) \\
\text{s.t. }& C_1\text{-}C_6,
\end{aligned}$$

and a rank-constrained linear programming problem,

$$\begin{aligned}
(\mathcal{P}3)\ \max_{\boldsymbol{P}}\ & E(\mathbf{P}) \\
\text{s.t. }& C_4\text{-}C_7,
\end{aligned}$$

where $\mathcal{P}2$ first determines the assignment of RBs for each BS at different time blocks and $\mathcal{P}3$ then takes as input the RB assignment and allocate power to satisfy the rank constraint.

C. Solution to $\mathcal{P}2$

We want to use the Dinkelbach's method [23] to solve $\mathcal{P}2$, which requires the concavity of the objective function and convexity of the constraints. To satisfy these requirements, we need to transform the fractional objective function, relax the binary variables, and approximate the non-convex items.

1) Transformation of the Fractional Objective: We first transform the fractional objective into a substractive form. After the transformation, the objective function becomes

$$\max_{\boldsymbol{P},\boldsymbol{\delta}}\ f(\mathbf{P}) - \lambda g(\mathbf{P}), \tag{4}$$

where λ is initialized to a feasible solution for energy efficiency and updated after each iteration until convergence. Since the Dinkelbach's method requires the concavity of $f(\mathbf{P})$, the convexity of $g(\mathbf{P})$, and the convexity of the feasible set, we need to solve the non-concavity issue in the objective function and the non-convexity issue in the constraints.

2) Continuous Relaxation: We eliminate the mixed-integer property of the original problem by converting the binary variables $\delta_{k,z}[d][l]$ into continuous variables between 0 and 1. To ease the conversion from the relaxed continuous variables back to binary numbers, we introduce a penalty term in the objective function pushing $\delta_{k,z}[d][l]$ towards 0 or 1. After adding this penalty term, we rewrite objective function as

$$\begin{aligned}
\max_{\boldsymbol{P},\boldsymbol{\delta}}\ & f(\mathbf{P}) - \lambda g(\mathbf{P}) \\
& + \xi \sum_{k\in\mathcal{K}}\sum_{z\in\mathcal{U}_k}\sum_{d\in\mathcal{RB}_k}\sum_{l\in\mathcal{T}}\delta_{k,z}[d][l](\delta_{k,z}[d][l]-1).
\end{aligned}$$

3) Convex Approximation: We want to solve the non-concavity issue in the objective function and the non-convexity issue in the constraint C_4. We rewrite $f(\mathbf{P})$ using the D.C. decomposition [24] as

$$f(\mathbf{P}) = f_1(\mathbf{P}) - f_2(\mathbf{P}),$$

where

$$\begin{aligned}
f_1(\mathbf{P}) &= \sum_{k\in\mathcal{K}}\sum_{z\in\mathcal{U}_k}\sum_{d\in\mathcal{RB}_k}\sum_{l\in\mathcal{T}} log(q(\mathbf{P})), \\
f_2(\mathbf{P}) &= \sum_{k\in\mathcal{K}}\sum_{z\in\mathcal{U}_k}\sum_{d\in\mathcal{RB}_k}\sum_{l\in\mathcal{T}} log(q(\mathbf{P}) - p_k[d][l]s_{(k,d),(z,d)}), \\
q(\mathbf{P}) &= \sum_{k'\in\mathcal{K}}\sum_{d'\in\mathcal{RB}_{k'}} p_{k'}[d'][l]s_{(k',d'),(z,d)} + V.
\end{aligned}$$

TABLE I
SIMULATION PARAMETERS

#UEs per BS	3	Cell radius	250m
Time slot length	1ms	Max. BS power	30dbm
Carrier freq. (f_c)	3.5GHz	Noise spectrum	-174dBm/Hz
SCS	{15,30}kHz	Max. UE power	20dbm

We define

$$f_1(\mathcal{P},\boldsymbol{\delta})=f_1(\mathbf{P})-\lambda g(\mathbf{P})-\xi(\sum_{k\in\mathcal{K}}\sum_{z\in\mathcal{U}_k}\sum_{d\in\mathcal{RB}_k}\sum_{\beta\in\mathcal{T}}\delta_{kz}[d][l]),$$
$$f_2(\mathcal{P},\boldsymbol{\delta})=f_2(\mathbf{P})-\xi(\sum_{k\in\mathcal{K}}\sum_{z\in\mathcal{U}_k}\sum_{d\in\mathcal{RB}_k}\sum_{l\in\mathcal{T}}\delta_{kz}[d][l]^2),$$

and rewrite the objective function as

$$\max_{\boldsymbol{P},\boldsymbol{\delta}}\ f_1(\mathbf{P},\boldsymbol{\delta})-f_2(\mathbf{P},\boldsymbol{\delta}).$$

To make the objective function concave, $f_2(\mathbf{P},\boldsymbol{\delta})$ should be transformed to be affine by employing the first-order Taylor approximation, i.e.,

$$\begin{aligned}\widetilde{f}_2(\mathbf{P},\boldsymbol{\delta})\triangleq&f_2(\mathbf{P}^{(t-1)},\boldsymbol{\delta}^{(t-1)})\\&+\nabla^T_{f_2}(\mathbf{P}^{(t-1)},\boldsymbol{\delta}^{(t-1)})[(\mathbf{P},\boldsymbol{\delta})-(\mathbf{P}^{(t-1)},\boldsymbol{\delta}^{(t-1)})].\end{aligned}$$

To relax C_4, we first decompose it into two constraints, i.e.,

$$(C_{4.1})\ G_{k,z}[d][l]=\sum_{k'\in\mathcal{K},d'\in\mathcal{RB}_{k'}}p_{k'}[d'][l]s_{(k',d'),(z,d)}-p_k[d][l]s_{(k,d),(z,d)}+V$$

and

$$(C_{4.2})\ \frac{p_k[d][l]}{\gamma_{k,z}}s_{(k,d),(z,d)}\geq\delta_{k,z}[d][l]G_{k,z}[d][l].$$

We use the successive convex approximation (SCA) to convert $C_{4.2}$ to

$$(C_{4.3})\ \frac{p_k[d][l]}{\gamma_{k,z}}s_{(k,d),(z,d)}\geq\frac{\phi_{k,z}[d][l]}{2}\delta_{k,z}[d][l]^2+\frac{G_{k,z}[d][l]^2}{2\phi_{k,z}[d][l]},$$

where $\phi_{k,z}[d][l]$ is a constant larger than 0 and the equality holds when $\phi_{k,z}[d][l]=\frac{G_{k,z}[d][l]}{\delta_{k,z}[d][l]}$.

Combining all the above operations, we can rewrite $\mathcal{P}2$ as

$$\begin{aligned}(\mathcal{P}2^*)\ \max_{\mathbf{P},\boldsymbol{\delta},\mathbf{G}}\ &f_1(\mathbf{P},\boldsymbol{\delta})-\widetilde{f}_2(\mathbf{P},\boldsymbol{\delta})\\\text{s.t. }&C_1,C_2,C_{4.1},C_{4.3},C_5,C_6,\\&\delta_{k,z}[d][l]\in[0,1],\forall k,z,d,l\end{aligned}$$

where $\mathbf{G}$ represents for variables $G_{k,z}[d][l]$'s. It can be seen that $\mathcal{P}2^*$ is a second-order cone programming (SOCP) problem. The solution to the original problem $\mathcal{P}2$ can be achieved by iteratively solving $\mathcal{P}2^*$ until convergence.

D. Solution to $\mathcal{P}3$

After $\boldsymbol{\delta}$ is determined, C_4 becomes a linear constraint and $\mathcal{P}3$ degenerates to a rank-constrained linear programming problem. We can rewrite $\mathcal{P}3$ as

$$\begin{aligned}(\mathcal{P}3^*)\ \max_{\mathbf{P}}\ &f_1(\mathbf{P},\hat{\boldsymbol{\delta}})-\widetilde{f}_2(\mathbf{P},\hat{\boldsymbol{\delta}})\\\text{s.t. }&C_4\text{-}C_7.\end{aligned}$$

As shown in [25], rank-constrained problems can be gradually approximated with a sequence of semidefinite programming (SDP) problems. Specifically, we have $rank(\boldsymbol{P})=N_{RB}$ if and only if there exists a $\boldsymbol{Z}\in\mathbb{S}^n$ such that

$$\boldsymbol{U}=\begin{bmatrix}\boldsymbol{I}_{N_{RB}}&\boldsymbol{P}^T\\\boldsymbol{P}&\boldsymbol{Z}\end{bmatrix},V_p^T\boldsymbol{Z}V_p>0,\text{ and }e\boldsymbol{I}_n-\boldsymbol{W}^T\boldsymbol{U}\boldsymbol{W}\succeq0,$$

where $\mathbb{S}^n$ is the set of symmetric $n\times n$ matrices, $V_p\in\mathbb{R}^{n\times1}$ is the eigenvector corresponding to the $(n-N_{RB}+1)$-th smallest eigenvalue of $\boldsymbol{Z}$, and $\boldsymbol{W}\in\mathbb{R}^{(n+N_{RB})\times n}$ are the eigenvectors corresponding to the n smallest eigenvalues of $\boldsymbol{U}$.

With the SDP approximations, we can solve $\mathcal{P}3^*$ by iteratively solving the following problem:

$$\max_{\mathbf{P}^{(t)},\boldsymbol{Z}^{(t)},e^{(t)}}f_1(\mathbf{P}^{(t)},\hat{\boldsymbol{\delta}})-\widetilde{f}_2(\mathbf{P}^{(t)},\hat{\boldsymbol{\delta}})-w^{(t)}e^{(t)}\quad(5a)$$
$$\text{s.t.}\quad\left(V_p^{(t-1)}\right)^T\boldsymbol{Z}^{(t)}V_p^{(t-1)}>0\quad(5b)$$
$$e^{(t)}\boldsymbol{I}_n-\left(\boldsymbol{W}^{(t-1)}\right)^T\boldsymbol{U}^{(t)}\boldsymbol{W}^{(t-1)}\succeq0\quad(5c)$$
$$0\leq e^{(t)}\leq e^{(t-1)}\quad(5d)$$
$$\boldsymbol{Z}^{(t)}\succeq\mathbf{0},\boldsymbol{U}^{(t)}\succeq\mathbf{0},\quad(5e)$$
$$C_4,C_5,C_6\quad(5f)$$

where $\mathbf{P}^{(t)}$ is the transmit power matrix at the t-th iteration, $\boldsymbol{W}^{(t-1)}$ includes the eigenvectors of $\boldsymbol{U}^{(t-1)}$, and $w^{(t)}$ is a weighting factor increasing with t. At the 0-th iteration, the initial solution can be obtained by solving the problem without constraints (5b)-(5d), and $e^{(0)}$ is the n-th smallest eigenvalue of $\boldsymbol{U}^{(0)}$.

V. PERFORMANCE EVALUATION

We evaluate the performance of our proposed joint optimization via simulations. The simulation parameters are selected to simulate a typical 5G multi-cell multi-numerology system, as listed in Table I. Our experimental setup consists of 3 hexagonal cells, each with one BS located in the center. Each cell contains 3 randomly located UEs. Neighboring cells are 500 meters apart. The UMi-Street Canyon NLoS model is used to calculate path-loss (PL) as $PL(d)=22.4+35.3\log_{10}(d)+21.3\log_{10}(f_c)$, where f_c is the carrier frequency and d is the distance. Small-scale fading is considered with the channel gains following an exponential distribution with a unit mean. The modulation and coding schemes (MCSs) and the corresponding SINR requirements are chosen randomly for UEs.

Convergence Performance. We evaluate the convergence performance of our proposed approach under random topologies. Fig. 2 shows the convergence process of our approach under a random topology, where it takes about 10 iterations for our

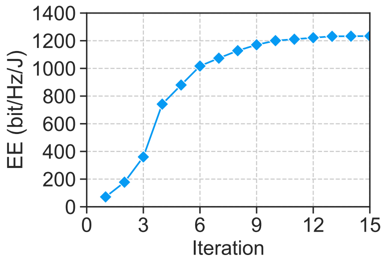

Fig. 2. Convergence performance

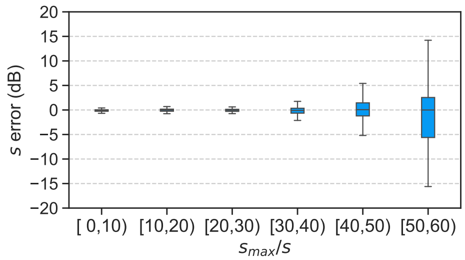

Fig. 3. Accuracy of estimated channel gains

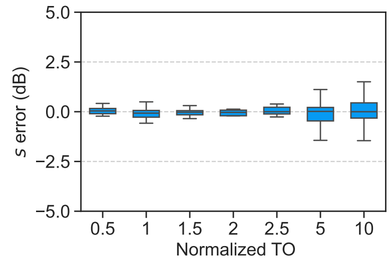

Fig. 4. Robustness to timing offset (TO)

approach to converge to a feasible solution. This indicates that our iterative approach is convergent.

Channel Gain Estimation. Let $s_{(k',d'),(z,d)}$ and $\hat{s}_{(k',d'),(z,d)}$ denote the actual and estimated equivalent channel gains from RB d' of BS k' to RB d of UE z, respectively. We use the logarithmic error, calculated as $10\log_{10}\left(\hat{s}_{(k',d'),(z,d)}/s_{(k',d'),(z,d)}\right)$ in dB, to measure the accuracy of channel gain estimation, where the error is zero when the estimated and actual channel gains are equal. Fig. 3 shows the estimation errors for channel gains of different magnitudes, where the magnitude is relative to the maximum channel gain in the network, denoted as s_{max}. It can be seen that the estimation error (s error) increases as the equivalent channel gain decreases and that the equivalent channel gains can be accurately estimated even when they are 50dB less than s_{max}. Although weak interference channels are likely to experience larger estimation errors, their influence on the resulting interference is very limited due to small channel gains. The interference experienced by UEs on different RBs can thus be accurately estimated.

Robustness to TO. Fig. 4 shows the estimation errors under different TOs, where the TO is normalized by the CP length of the OFDM symbol using the narrowest SCS. It can be seen that our approach can achieve very small estimation errors even when TO is twice larger than the CP length. The robustness of our approach to TO is because we conduct IGE in the power domain. Therefore, our approach outperforms the reference signal (RS)-based approach for IGE, which expects TO to be less than the CP length. More importantly, our approach can work with multiple numerologies, while the RS-based approach cannot effectively measure INI due to the misalignment of both the time and frequency domains among different numerologies.

Power overhead. Our approach introduces power as a new dimension for measuring interference channel gains and thus may incur additional power consumption. We compared our approach with the resource allocation scheme not considering IGE in terms of power consumption. Let P_1 and P_0 denote the power consumptions in our approach and the power resource allocation scheme, respectively. We define *power overhead* as $(P_1-P_0)/P_0$. Fig. 5 shows the distribution of power overheads under random topologies and different numbers of BSs from 3 to 7. It can be seen that the power overhead is less than 8% for almost all the experiments. Moreover, the power overhead decreases as the number of BSs increases because the extra power consumed by IGE increases slower than the total power consumption of the entire system.

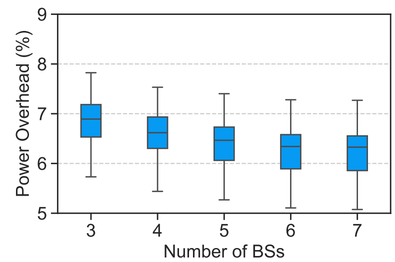

Fig. 5. Power overhead

VI. Conclusion

In this paper, we proposed a power-domain approach to estimate the interference graph, which is crucial for the resource allocation in multi-cell multi-numerology systems. Since our approach estimates the interference graph in power domain, it is robust to timing offset. We derived the linear relation between transmit/receive power and interference channel gains. Based on this relation, we provided the necessary condition for the feasibility of interference graph estimation and proposed to jointly optimize interference graph estimation and resource allocation. Simulation results show that the interference graph can be accurately estimated with low power overhead. For future work, we want to extend the joint optimization framework to other wireless networks.

VII. Acknowledgement

We appreciate the constructive feedback from the anonymous reviewers. This work was supported by the East China Branch of State Grid Corporation of China under the Grant 529924240006.

Appendix A
Proof of Lemma 1

Without loss of generality, we consider a multi-cell network with two numerologies i and i', where numerology i' has a larger SCS than numerology i and $T_i = 2^{i'}T_{i'}$. Based on Eq. (2) and $x_k[n] = \sum_{i\in\mathcal{I}_k} x_k^i[n]$, the frequency-domain received signal of UE z using numerology i can be expressed as

$$Y_z^i[d] = \frac{1}{\sqrt{N^i}} \sum_{k\in\mathcal{K}} \sum_{l=0}^{L-1} \sum_{n=0}^{N^i-1} h_{k,z}^{(l)} \sum_{i\in\mathcal{I}_k} x_k^i[n-l-\zeta_k] e^{-j\frac{2\pi(\omega_k-d)n}{N^i}}. \tag{7}$$

Let $X_{k,l}^i[d]$ be the symbol transmitted by BS k on subcarrier d of the l-th OFDM symbol in the least common multiplier

$$
\begin{aligned}
s_{(k,m),(z,d)}^{i'\to i} = \frac{1}{2^{\mu} N^i N^{i'}} \Bigg[& \left| \sum_{l=0}^{L-1} h_{k,z}^{(l)} e^{\frac{-j2\pi 2^{\mu} lm}{N^i}} \sum_{n=0}^{N_{tot}^{i}-N_{CP}^{i'}-1} e^{\frac{j2\pi(\Delta_{d,m}^{(i',i)}+\omega_k)n}{N^i}} \right|^2 + (2^{\mu}-2) \left| \sum_{l=0}^{L-1} h_{k,z}^{(l)} e^{\frac{-j2\pi 2^{\mu} lm}{N^i}} \sum_{n=0}^{N^{i'}-1} e^{\frac{j2\pi(\Delta_{d,m}^{(i',i)}+\omega_k)n}{N^i}} \right|^2 \\
& + \left| \sum_{l=0}^{L-1} h_{k,z}^{(l)} e^{\frac{-j2\pi 2^{\mu} lm}{N^i}} \sum_{n=0}^{N^{i'}-l-1} e^{\frac{j2\pi(\Delta_{d,m}^{(i',i)}+\omega_k)n}{N^i}} \right|^2 \Bigg].
\end{aligned} \tag{6}
$$

(LCM) duration. Since $\mathbb{E}[X_{k,l}^i[d]] = 0$ and $X_{k,l}^i[d]$'s are independent, we have that $\mathbb{E}[X_{k,l}^i[d] X_{k',l'}^{i'}[d']] \neq 0$ only if $i = i'$, $k = k'$, $l = l'$, and $d = d'$.

Let $\Delta_{d,m}^{i'\to i} = 2^{i'} m - d$, and $\Delta_{d,m}^{i\to i'} = m - 2^{i'} d$. From Eq. (7), we have that

$$
\begin{aligned}
2^{i'} \mathbb{E}[|Y_z^{i'}[d]|^2] = & \sum_{k\in\mathcal{K}} \sum_{m=0}^{N^{i'}-1} 2^{i'} \mathbb{E}[|X_k^{i'}[m]|^2] s_{(k,m),(z,d)}^{i'\to i'} \\
& + \sum_{k\in\mathcal{K}} \sum_{m=0}^{N^{i}-1} \mathbb{E}[|X_k^{i}[m]|^2] s_{(k,m),(z,d)}^{i\to i'} + \hat{V}_z[d],
\end{aligned}
$$

where

$$
s_{(k,m),(z,d)}^{i\to i} = \frac{1}{(N^i)^2} \left| \sum_{l=0}^{L-1} h_{k,z}^{(l)} \sum_{n=0}^{N^i-1} e^{\frac{j2\pi[(m+\omega_k-d)n-lm]}{N^i}} \right|^2,
$$

$$
s_{(k,m),(z,d)}^{i'\to i'} = \frac{2^{i'}}{(N^{i'})^2} \left| \sum_{l=0}^{L-1} h_{k,z}^{(l)} \sum_{n=0}^{N^{i'}-1} e^{\frac{j2\pi[(m+\omega_k-d)n-lm]}{N^{i'}}} \right|^2,
$$

$$
s_{(k,m),(z,d)}^{i\to i'} = \frac{2^{i'}}{N^i N^{i'}} \left| \sum_{l=0}^{L-1} h_{k,z}^{(l)} \sum_{n=0}^{N^{i'}-1} e^{\frac{j2\pi[(\Delta_{d,m}^{i\to i'}+2^{i'}\omega_k)n-lm]}{N^i}} \right|^2,
$$

where $s_{(k,m),(z,d)}^{i'\to i}$ is presented in Eq. (6).

Since $X_{k,l}^i[d]$'s are independent, we can easily extend the above derivation to cases with more than two numerologies and have that

$$
2^i \mathbb{E}[|Y_z^i[d]|^2] = \sum_{k\in\mathcal{K}} \sum_{j\in\mathcal{I}_k} \sum_{l=0}^{N^j-1} 2^j \mathbb{E}[|X_k^j[l]|^2] s_{(k,l)(z,d)}^{j\to i} + \hat{V}_z[d].
$$

References

[1] L. Zhang, P. Xiao, A. Zafar, A. ul Quddus, and R. Tafazolli, "FBMC system: An insight into doubly dispersive channel impact," *IEEE Trans. Veh. Technol.*, vol. 66, no. 5, pp. 3942–3956, 2016.

[2] B. Farhang-Boroujeny, "OFDM versus filter bank multicarrier," *IEEE Signal Processing Magazine*, vol. 28, no. 3, pp. 92–112, 2011.

[3] V. Vakilian, T. Wild, F. Schaich, S. ten Brink, and J.-F. Frigon, "Universal-filtered multi-carrier technique for wireless systems beyond LTE," in *Proceedings of the 2013 IEEE Globecom Workshops (GC Wkshps)*, 2013, pp. 223–228.

[4] N. Michailow, M. Matthé, I. S. Gaspar, A. N. Caldevilla, L. L. Mendes, A. Festag, and G. Fettweis, "Generalized frequency division multiplexing for 5th generation cellular networks," *IEEE Trans. Commun.*, vol. 62, no. 9, pp. 3045–3061, 2014.

[5] H. Chen, J. Hua, F. Li, F. Chen, and D. Wang, "Interference analysis in the asynchronous f-OFDM systems," *IEEE Trans. Commun.*, vol. 67, no. 5, pp. 3580–3596, 2019.

[6] E. Memisoglu, A. B. Kihero, E. Basar, and H. Arslan, "Guard band reduction for 5G and beyond multiple numerologies," *IEEE Commun. Lett.*, vol. 24, no. 3, pp. 644–647, 2019.

[7] L. Zhang, A. Ijaz, P. Xiao, M. M. Molu, and R. Tafazolli, "Filtered OFDM systems, algorithms, and performance analysis for 5G and beyond," *IEEE Trans. Commun.*, vol. 66, no. 3, pp. 1205–1218, 2017.

[8] M. Zambianco and G. Verticale, "Interference minimization in 5G physical-layer network slicing," *IEEE Trans. Commun.*, vol. 68, no. 7, pp. 4554–4564, 2020.

[9] A. Yazar and H. Arslan, "Reliability enhancement in multi-numerology-based 5G new radio using INI-aware scheduling," *EURASIP J. Wireless Commun. Netw.*, no. 110, pp. 1–14, 2019.

[10] L.-H. Shen, P.-Y. Wu, and K.-T. Feng, "Energy efficient resource allocation for multinumerology enabled hybrid services in B5G wireless mobile networks," *IEEE Trans. Wireless Commun.*, vol. 22, no. 3, pp. 1712–1729, 2022.

[11] X. Zhang, L. Zhang, P. Xiao, D. Ma, J. Wei, and Y. Xin, "Mixed numerologies interference analysis and inter-numerology interference cancellation for windowed OFDM systems," *IEEE Trans. Veh. Technol.*, vol. 67, no. 8, pp. 7047–7061, 2018.

[12] L. Zhang, A. Ijaz, P. Xiao, A. Quddus, and R. Tafazolli, "Subband filtered multi-carrier systems for multi-service wireless communications," *IEEE Trans. Wireless Commun.*, vol. 16, no. 3, pp. 1893–1907, 2017.

[13] H. Son, G. Kwon, H. Park, and J. S. Park, "Signal model and linear combining design for multi-numerology massive MIMO systems," *IEEE Trans. Veh. Technol.*, 2024.

[14] X. Cheng, R. Zayani, H. Shaiek, and D. Roviras, "Inter-numerology interference analysis and cancellation for massive MIMO-OFDM downlink systems," *IEEE Access*, vol. 7, pp. 177 164–177 176, 2019.

[15] T. V. S. Sreedhar and N. B. Mehta, "Inter-numerology interference in mixed numerology OFDM systems in time-varying fading channels with phase noise," *IEEE Trans. Wireless Commun.*, 2023.

[16] L.-H. Shen, C.-Y. Su, and K.-T. Feng, "CoMP enhanced subcarrier and power allocation for multi-numerology based 5G-NR networks," *IEEE Trans. Veh. Technol.*, vol. 71, no. 5, pp. 5460–5476, 2022.

[17] H. Elgendi, M. Mäenpää, T. Levanen, T. Ihalainen, S. Nielsen, and M. Valkama, "Interference measurement methods in 5G NR: Principles and performance," in *Proceedings of the 16th International Symposium on Wireless Communication Systems (ISWCS)*, 2019, pp. 233–238.

[18] H. Li, L. Han, R. Duan, and G. M. Garner, "Analysis of the synchronization requirements of 5G and corresponding solutions," *IEEE Communications Standards Magazine*, vol. 1, no. 1, pp. 52–58, 2017.

[19] W. Cui, K. Shen, and W. Yu, "Spatial deep learning for wireless scheduling," *IEEE Journal on Selected Areas in Communications*, vol. 37, no. 6, pp. 1248–1261, 2019.

[20] M. Lee, G. Yu, and G. Y. Li, "Graph embedding-based wireless link scheduling with few training samples," *IEEE Trans. Wireless Commun.*, vol. 20, no. 4, pp. 2282–2294, 2020.

[21] 3rd Generation Partnership Project (3GPP), "Physical channels and modulation," TS 38.211 version 17.1.0, Apr. 2022.

[22] K. T. K. Cheung, S. Yang, and L. Hanzo, "Achieving maximum energy-efficiency in multi-relay OFDMA cellular networks: A fractional programming approach," *IEEE Trans. Commun.*, vol. 61, no. 7, pp. 2746–2757, 2013.

[23] W. Dinkelbach, "On nonlinear fractional programming," *Manage. Sci.*, vol. 13, no. 7, pp. 492–498, 1967.

[24] H. H. Kha, H. D. Tuan, and H. H. Nguyen, "Fast global optimal power allocation in wireless networks by local DC programming," *IEEE Trans. Wireless Commun.*, vol. 11, no. 2, pp. 510–515, 2011.

[25] C. Sun and R. Dai, "Rank-constrained optimization and its applications," *Automatica*, vol. 82, pp. 128–136, 2017.